Article

Smad6/Smurf1 overexpression in cartilage delays chondrocyte hypertrophy and causes dwarfism with osteopenia

Mitsuru Horiki,[1] Takeshi Imamura,[2] Mina Okamoto,[1] Makoto Hayashi,[2] Junko Murai,[1] Akira Myoui,[1] Takahiro Ochi,[1] Kohei Miyazono,[2,3] Hideki Yoshikawa,[1] and Noriyuki Tsumaki[1]

[1]Department of Orthopaedics, Osaka University Graduate School of Medicine, Osaka 565-0871, Japan
[2]Department of Biochemistry, The Cancer Institute of the Japanese Foundation for Cancer Research, Tokyo 170-8455, Japan
[3]Department of Molecular Pathology, Graduate School of Medicine, University of Tokyo, Tokyo 113-0033, Japan

Biochemical experiments have shown that Smad6 and Smad ubiquitin regulatory factor 1 (Smurf1) block the signal transduction of bone morphogenetic proteins (BMPs). However, their in vivo functions are largely unknown. Here, we generated transgenic mice overexpressing Smad6 in chondrocytes. Smad6 transgenic mice showed postnatal dwarfism with osteopenia and inhibition of Smad1/5/8 phosphorylation in chondrocytes. Endochondral ossification during development in these mice was associated with almost normal chondrocyte proliferation, significantly delayed chondrocyte hypertrophy, and thin trabecular bone. The reduced population of hypertrophic chondrocytes after birth seemed to be related to impaired bone growth and formation. Organ culture of cartilage rudiments showed that chondrocyte hypertrophy induced by BMP2 was inhibited in cartilage prepared from Smad6 transgenic mice. We then generated transgenic mice overexpressing Smurf1 in chondrocytes. Abnormalities were undetectable in Smurf1 transgenic mice. Mating Smad6 and Smurf1 transgenic mice produced double-transgenic pups with more delayed endochondral ossification than Smad6 transgenic mice. These results provided evidence that Smurf1 supports Smad6 function in vivo.

Introduction

Bone morphogenetic proteins (BMPs) were originally identified as secreted signaling molecules that could induce ectopic endochondral bone formation when implanted subcutaneously. Subsequent molecular cloning experiments have revealed that the BMP family consists of various molecules including the growth and differentiation factor subfamily, and belongs to the TGF-β superfamily. BMP family members have diverse biological activities during the development of various organs and tissues, as well as during embryonic axis determination (Hogan, 1996).

Members of the TGF-β superfamily transduce their signals through two types of serine/threonine kinase receptors, types I and II (Heldin et al., 1997; Shi and Massague, 2003). Upon ligand binding, type I and type II receptors form a tetramer consisting of two pairs of type I and type II receptors.

Type II receptors phosphorylate type I receptors. Then, type I receptors phosphorylate downstream targets such as Smads. In vertebrates, seven type I receptors and five type II receptors have been found so far. Among them, three type I receptors, BMP type IA receptor (BMPR-IA, or activin receptor-like kinase [ALK-3]), BMPR-IB (ALK-6), and ALK-2, mediate BMP signaling. Smads are the major downstream targets of type I receptors for TGF-β/BMP superfamily proteins (Heldin et al., 1997). Eight Smads have been identified in mammals and are classified into three subgroups. Receptor-regulated Smads (R-Smads) are phosphorylated at SSXS motifs at their COOH terminus by type I receptors. Smad1, Smad5, and Smad8 are R-Smads that transduce BMP signals, and Smad2 and Smad3 are responsible for TGF-β and activin signaling. Phosphorylated R-Smads form heteromers with

Address correspondence to Noriyuki Tsumaki, Dept. of Orthopaedics, Osaka University Graduate School of Medicine, 2-2 Yamadaoka, Suita, Osaka 565-0871, Japan. Tel.: 81-6-6879-3552. Fax: 81-6-6879-3559. email: tsumaki-n@umin.ac.jp

Key words: chondrocyte; hypertrophy; osteopenia; dwarfism; transgenic mice

Figure 1. **Postnatal dwarfism in Smad6 transgenic mice.** (A) Diagram of DNA constructs used to generate Smad6 transgenic mice. Gene structure of *Col11a2* is shown at top. Boxes indicate coding regions and solid lines denote noncoding sequences. A 1.6-kb DNA fragment covering the entire coding region of mouse Smad6 cDNA tagged with FLAG sequence at the 5′ terminus was ligated to the promoter and 1st intron enhancer sequences of the *Col11a2* gene. Bracket indicates SV40 splice cassette. (B) Normal and transgenic pups from lines 138 and 139 at 3 wk of age. (C) RT-PCR analysis of Smad6 mRNA expression at 16.5 d.p.c. (D and E) Temporal changes in crown–rump length (D) and weight (E) of wild-type and Smad6 transgenic mice from line 199 (n = 12). (F–H) Length of humerus (F), femur (G), and tibia (H) in wild-type and Smad6 transgenic mice from line 199 at 3 wk of age (n = 5). Error bars show means ± SD. *, P < 0.01 between wild-type and transgenic mice as determined by *t* test. Bar (B), 3 cm.
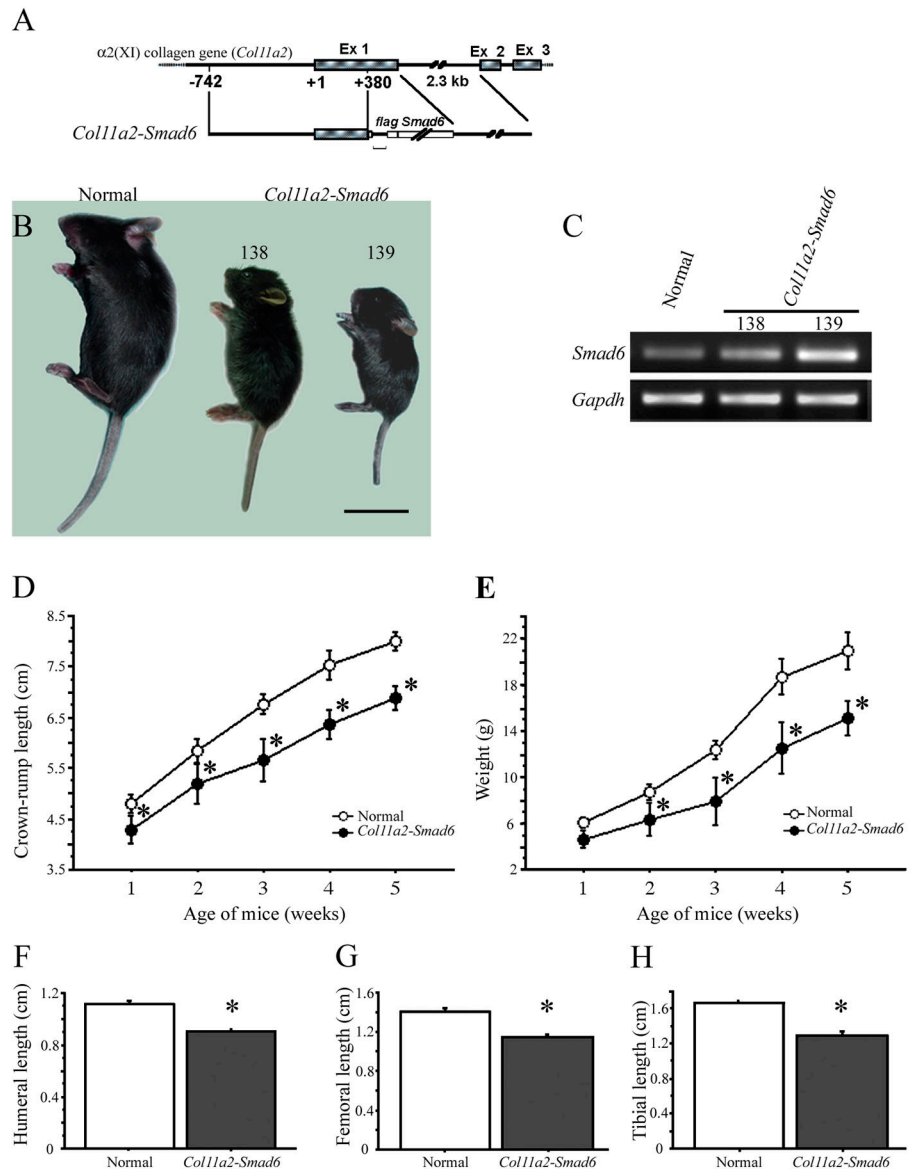
the common-partner Smad (Smad4), and translocate into the nucleus where they interact with transcriptional factors to bind directly or indirectly to specific DNA sequences for the activation of gene transcription.

BMP signaling is subject to delicate regulation at multiple levels: extracellularly, at the membrane site, and intracellularly (Balemans and Van Hul, 2002). In the extracellular space, several molecules antagonize BMPs. Among these antagonists, noggin is expressed in cartilage and binds to BMPs and prevents them from interacting with their receptors. At the intracellular level, inhibitory Smads, Smad6 and Smad7, inhibit phosphorylation of R-Smads by competing with R-Smads for binding to phosphorylated type I receptors. In particular, Smad6 appears to inhibit BMP signaling, whereas Smad7 associates stably with TGF-β receptor and BMP receptor complexes and inhibits the TGF-β– or BMP-mediated phosphorylation of R-Smads (Hanyu et al., 2001). In addition, ubiquitin-dependent protein degradation plays key roles in Smad signaling. Smad ubiquitin regulatory factor 1 (Smurf1) and Smurf2 induce the ubiquitination and degra-

dation of Smad1 and Smad5 (Zhu et al., 1999; Zhang et al., 2001). Furthermore, Smurf1 and Smurf2 interact with nuclear Smad7 and induce the nuclear export of Smad7. Smurf–Smad7 complexes then associate with type I receptor for TGF-β and enhance its turnover (Kavsak et al., 2000; Ebisawa et al., 2001). Recent biochemical analyses have shown that Smurf1 binds to BMP type I receptors via Smad6 and Smad7, and that it induces the ubiquitination and degradation of these receptors (Murakami et al., 2003). Thus, Smad6 and Smurf1 cooperatively down-regulate BMP signals by degradation of R-Smads as well as BMP receptors. However, the physiological function of Smurfs is unknown.

During development, the limb skeleton is formed through endochondral bone formation (Erlebacher et al., 1995). Mesenchymal cells initially undergo condensation followed by differentiation of cells within these condensations into chondrocytes. Chondrocytes then proliferate and produce ECM to form primordial cartilage. Shortly after the primordial cartilage formation, proliferating chondrocytes in the central region of the cartilage undergo terminal differentia-

tion to hypertrophic chondrocytes. Hypertrophic chondrocytes exit the cell cycle and synthesize an ECM that is different in composition from that of proliferating cartilage. The hypertrophic cartilage is invaded by blood vessels along with osteoblasts, osteoclasts, and hematopoietic cells to form primary ossification centers. Within these centers, the hypertrophic cartilage matrix is degraded, hypertrophic chondrocytes die, and osteoblasts replace the disappearing cartilage with trabecular bone (Olsen et al., 2000). Then, bone formation and maintenance are performed by a balance between the new apposition of bony matrix by osteoblasts and resorption by osteoclasts.

Smad proteins have been identified in growth plate cartilage (Flanders et al., 2001). In vitro analyses have shown that Smad6 regulates the chondrocytic phenotype (Valcourt et al., 2002; Nishihara et al., 2003). However, the physiological roles of Smad6 and Smad signaling in normal endochondral bone formation have not been determined. Here, we generated transgenic mice overexpressing Smad6 or Smurf1 in chondrocytes under the control of the $\alpha2(XI)$ collagen chain gene (*Col11a2*) promoter/enhancer sequences. We found that overexpression of Smad6 does not significantly affect chondrocyte proliferation, but significantly delays chondrocyte hypertrophy, which may lead to postnatal dwarfism with osteopenia. By using double-transgenic mice, we also found that Smurf1 supports Smad6 function in vivo.

Results

Generation of Smad6 transgenic mouse lines

We ligated the Smad6 cDNA with a 5′ FLAG epitope to *Col11a2* promoter/enhancer sequences to construct the transgene *Col11a2-Smad6* (Fig. 1 A). Generation zero (G$_0$) embryos of Smad6 transgenic mice were initially killed, in case Smad6 transgenic mice were lethal. 17 of 129 embryos were genetically positive for the transgene. Smad6 transgenic and normal embryos appeared similar. The Smad6 transgenic mice survived after birth, so several independent transgenic mouse lines could be established. The phenotypes of all transgenic mouse lines were similar, with differences in the degree of abnormalities between lines.

Postnatal dwarfism in Smad6 transgenic mice

1 wk after birth, the Smad6 transgenic mice started to develop dwarfism (Fig. 1, B–H). Our data were collected from three transgenic founders derived from microinjections, transgenic pups with severe phenotypes generated from two mosaic founders (lines 138 and 139), and transgenic offspring with mild phenotypes generated from two transgenic founders (lines 165 and 199). Dwarfism was more severe in the transgenic mice of line 139 than of line 138 (Fig. 1 B). Phenotype severity closely correlated with transgene expression levels as shown by RT-PCR (Fig. 1 C). Quantitative real-time RT-PCR using total RNAs extracted from limb buds showed that the amount of Smad6 mRNAs of transgenic line 139 was threefold that of normal mice, and double that of transgenic line 138. At 3 wk after birth, the average crown–rump length of transgenic mice (line 199) was ~20% shorter than that of normal mice (Fig. 1 D). Transgenic mice (line 199) weighed an average of 30–40% less (Fig. 1 E), and
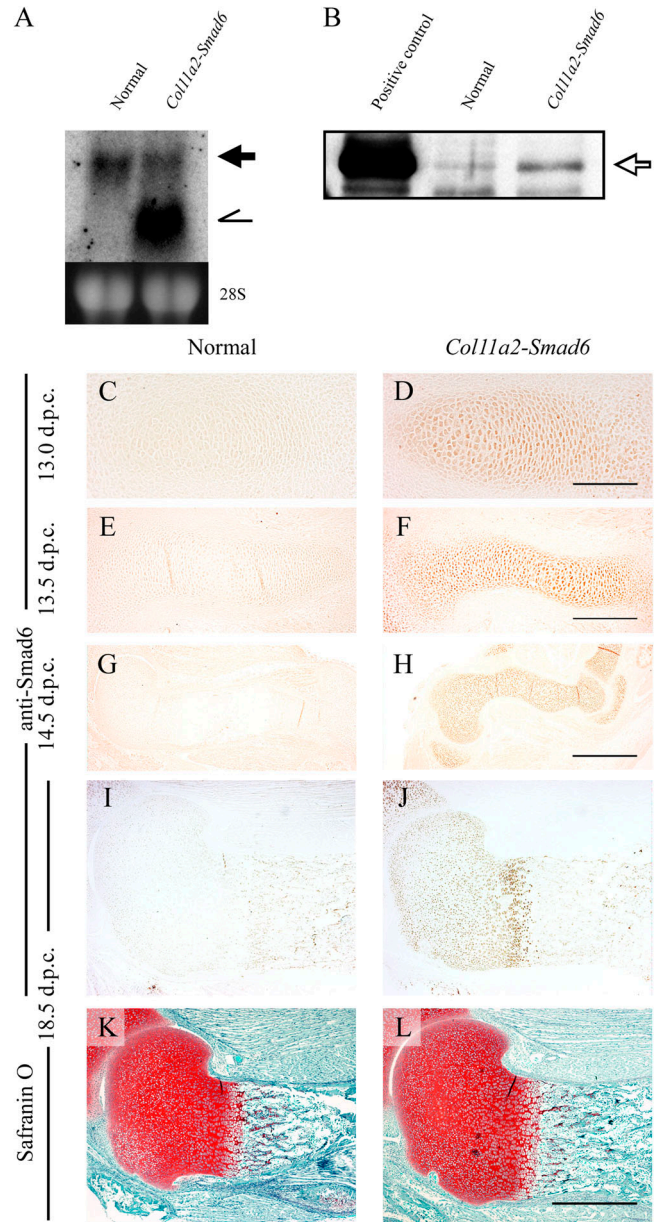

Figure 2. **Cartilage-specific expression of transgene in Smad6 transgenic mice.** (A) Northern blot hybridized with Smad6 probe. Bottom shows ethidium bromide–stained gel before transfer. (B) Protein expression of Smad6 transgene. Positive control consisted of lysates from COS7 cells transfected with expression construct FLAG-Smad6 (left lane). (C–L) Immunohistochemical analysis of humerus from normal (C, E, G, and I) and Smad6 (D, F, H, and J) transgenic mice at various stages of development using anti-Smad6 antibody. Serial sections for I and J were stained with safranin O/fast green/iron hematoxylin (K and L). Arrow indicates endogenous Smad6 mRNA. Half-arrow indicates Smad6 transgene mRNA. Open arrow represents FLAG-tagged Smad6 protein. Bars: (C and D) 100 μm; (E and F) 200 μm; (G–L) 500 μm.

the average length of the skeletal components was 20–30% shorter compared with normal littermates (Fig. 1, F–H).

Cartilage-specific expression of transgene in Smad6 transgenic mice

Northern blotting demonstrated Smad6 expression in the limb buds of transgenic mice. Transgene Smad6 mRNA was
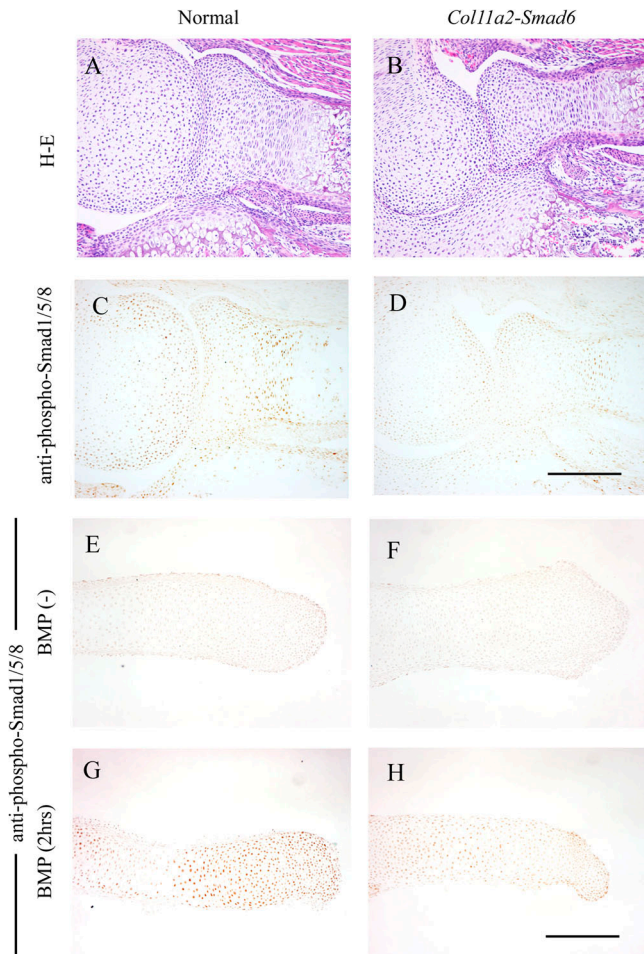
Normal   *Col11a2-Smad6*

Figure 3. **Blockage of Smad signaling in cartilage of Smad6 transgenic mice.** (A–D) Immunohistochemistry of elbow joints in wild-type (A and C) and transgenic (B and D) mice at 16.5 d.p.c. Staining with hematoxylin and eosin (A and B). Serial sections of A and B were immunostained using anti-phospho-Smad1/5/8 antibody (C and D). (E–H) Immunohistochemistry of metatarsal cartilage explants at 15.0 d.p.c. before (E and F) and after exposure to rhBMP2 for 2 h (G and H). Phospho-Smad1/5/8 immunoreactivity was not increased by rhBMP2 in sections of cartilage explants from Smad6 transgenic mice (F and H) compared with those in wild-type mice (E and G). Bars: (A–D) 300 μm; (E–H) 200 μm.

~2 kb in length, which was smaller than endogenous Smad6 mRNA due to shorter 5′ and 3′ untranslated regions (Fig. 2 A). Immunoblotting demonstrated the expression of a 70-kD FLAG-tagged Smad6 protein in limb buds of Smad6 transgenic mice (Fig. 2 B, open arrow). Immunohistochemistry using anti-Smad6 antibody showed more intense signals for Smad6 proteins in forelimb chondrocytes of Smad6 transgenic mice (Fig. 2, D, F, H, and J) than from wild-type mice (Fig. 2, C, E, G, and I) from 13.0 through 18.5 days post coitus (d.p.c.).

Blockage of Smad signaling in cartilage of Smad6 transgenic mice

We examined Smad signaling in chondrocytes by immuno-histochemistry using an antibody that recognizes only phosphorylated forms of Smad1, Smad5, and Smad8. Phospho-Smad1/5/8 immunoreactivity was reduced in transgenic

cartilage sections from 16.5 d.p.c. limbs (Fig. 3, B and D) compared with the wild type (Fig. 3, A and C). We cultured explants of metatarsal primordial cartilage from 15.0 d.p.c. embryos. Recombinant human BMP2 (rhBMP2) proteins were added to the culture media and explants were histologically analyzed 2 h later. rhBMP2 dramatically increased phospho-Smad1/5/8 immunoreactivity in explants from wild-type mice (Fig. 3, E and G), but not from Smad6 transgenic mice (Fig. 3, F and H). These results suggested that Smad signaling was inhibited in the transgenic cartilage by an excess of Smad6.

Osteopenia in Smad6 transgenic mice

We analyzed the bone structure of transgenic mice. Micro-CT analysis of the humerus revealed that the primary spongiosa was significantly more hypoplastic and disorganized in Smad6 transgenic mice (Fig. 4, B and D) than in normal littermates (Fig. 4, A and C). The average bone volume per total tissue volume of primary spongiosa was 30–40% smaller than that of normal littermates (Fig. 4 E).

Differences in bone formation were further examined by bone histomorphometric analysis. Trabecular bone volume was significantly decreased in Smad6 transgenic mice (Fig. 4 F). The osteoblast surface per bone surface in transgenic mice was significantly decreased (Fig. 4 G). We analyzed dynamic changes in bone formation and mineralization by injecting tetracycline and calcein at 2-d intervals. The distance between the two consecutive labels was significantly decreased in transgenic mice (Fig. 4, H–J). The mineralization surface was decreased, although not significantly (Fig. 4 K). These data showed a significantly decreased bone formation rate (Fig. 4 L). As for osteoclastic bone resorption, the osteoclast number per bone surface, osteoclast surface per bone surface, and erosive surface per bone surface were significantly increased (Fig. 4, M–O).

To elucidate the mechanism by which osteoclastic bone resorption was activated in Smad6 transgenic mice, we performed bone marrow cell culture and analyzed dexamethasone/parathyroid hormone–induced osteoclastogenesis. The number of tartrate-resistant acid phosphatase (TRAP)–positive multinucleated cells in the culture prepared from transgenic mice was equivalent to that of normal mice (Fig. 4, P–R). The resorption of hydroxyapatite by cultured osteoclast prepared from transgenic mice was essentially normal (Fig. 4 S). Next, we examined osteoclast formation activities in spleen cell culture in the presence of RANK ligand. RANK ligand–induced osteoclastogenesis of spleen cells from Smad6 transgenic mice was normal, as indicated by the number of TRAP-positive multinucleated cells and the resorption of hydroxyapatite (unpublished data). These results suggested that both osteoclast precursors and osteoclast-supporting activities of osteoblast/stromal cells were normal in the bone marrow of Smad6 transgenic mice.

Skeletal development of Smad6 transgenic mice

Because the transgene was expressed specifically in cartilage, we analyzed the skeleton from earlier stages of development. Whole-mount in situ hybridization using a type II collagen gene (*Col2a1*) antisense cRNA probe showed that the pattern and intensity of signals did not obviously differ between
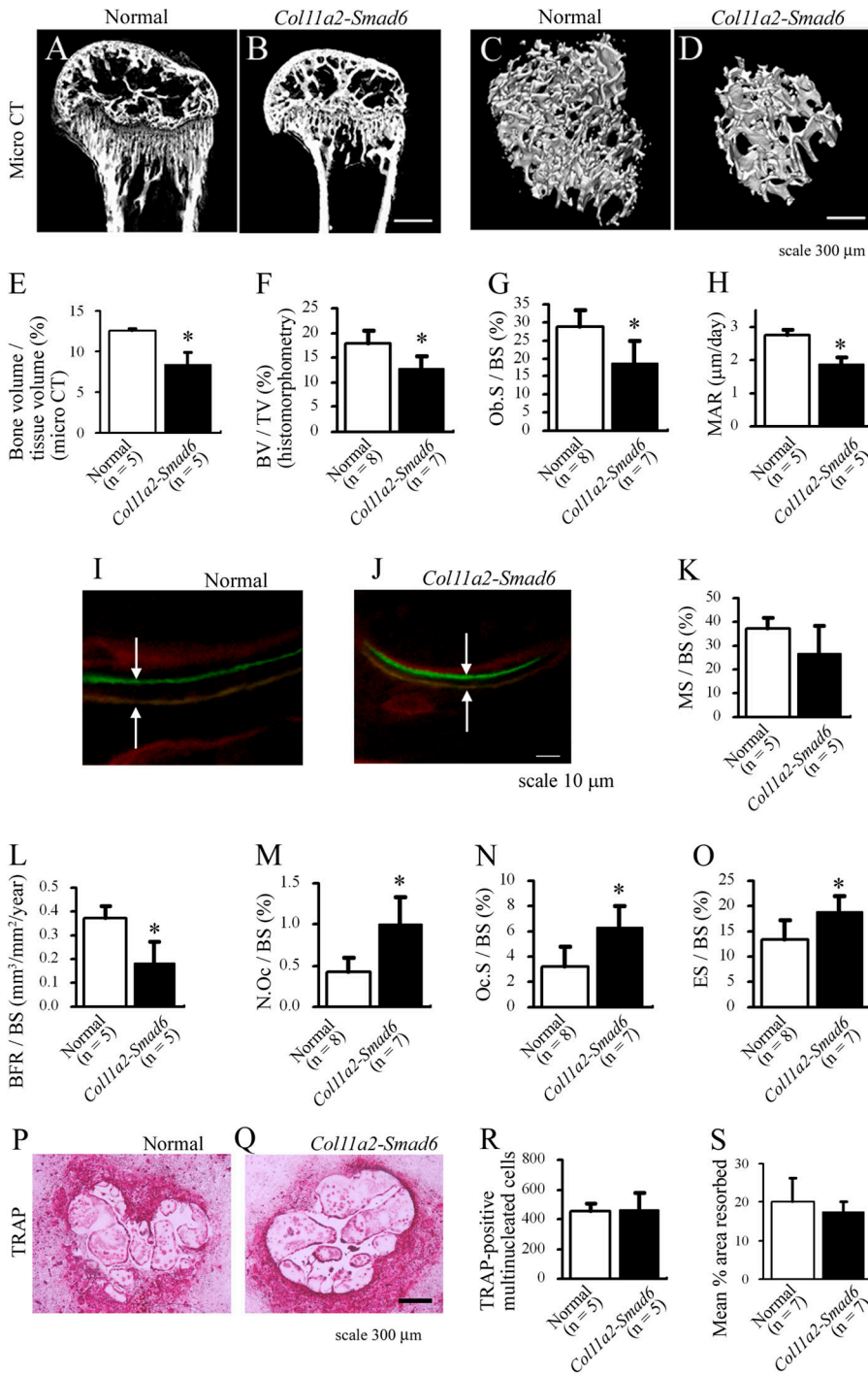
Figure 4. **Osteopenia in Smad6 transgenic mice.** (A–E) Micro-CT analysis of proximal humerus in 3-wk-old normal (A and C) and Smad6 transgenic (B and D) mice. Reconstructed coronal view (A and B) and reconstructed three-dimensional image (C and D) of trabecular bone. (E) Trabecular bone volume per total tissue volume compared between normal and transgenic mice. (F–O) Bone histomorphometric analysis of fourth lumbar vertebral bodies at 4 wk of age. (F) Trabecular bone volume (BV/TV; bone volume over tissue volume), (G) osteoblast surface per bone surface (Ob.S/BS), (H) mineral apposition rate (MAR), (K) mineralizing surface per bone surface (MS/BS), (L) bone-forming rate per bone surface (BFR/BS), (M) osteoclast number per bone surface (N.Oc/BS), (N) osteoclast surface per bone surface (Oc.S/BS), and (O) eroded surface per bone surface (ES/BS) compared between normal and transgenic mice. Fluorescent micrograph of labeled mineralization fronts in normal (I) and Smad6 transgenic (J) mice. (P–S) Osteoclastogenesis of cultured bone marrow cells. Micrograph of cultured multinucleated cells stained with TRAP prepared from normal (P) and Smad6 transgenic (Q) mice. Number of TRAP-positive multinucleated cells (R) and resorption of hydroxyapatite (S) were compared between normal and transgenic mice. Error bars show means ± SD. *, $P < 0.01$ between normal and transgenic mice as determined by t test. Bars: (A–D, P, and Q) 300 μm; (I and J) 10 μm.

Smad6 transgenic and normal mice at either 12.5 (Fig. 5, A and B) or 13.0 (Fig. 5, C and D) d.p.c. This suggested that mesenchymal condensation was essentially normal in the transgenic mice. At 13.5 d.p.c., the size and shape of each cartilaginous skeletal component stained with Alcian blue of transgenic mice were essentially identical to those of normal littermates (Fig. 5, E and F). The central regions of metatarsals were mineralized in normal mice as they were stained with Alizarin red S, but not in transgenic mice at 16.5 d.p.c. (Fig. 5, G and H, arrowheads) and at 18.5 d.p.c. (Fig. 5, I and J, arrowheads). The size of mineralized tissue in the humerus and femur was considerably smaller in transgenic

mice than in normal mice (Fig. 5, G and H, arrows). At 3 wk of age, skeleton of transgenic mice was much smaller than that of normal mice (Fig. 5, K and L).

Delayed hypertrophy of chondrocytes in Smad6 transgenic mice

We further examined endochondral bone formation by histological means. At 13.5 d.p.c. when condensed mesenchymal cells differentiate into chondrocytes, chondrocytes did not obviously differ histologically between normal and transgenic mice (Fig. 6, A and B). At 14.5 d.p.c., proliferative chondrocytes exit the cell cycle and start terminal differ-
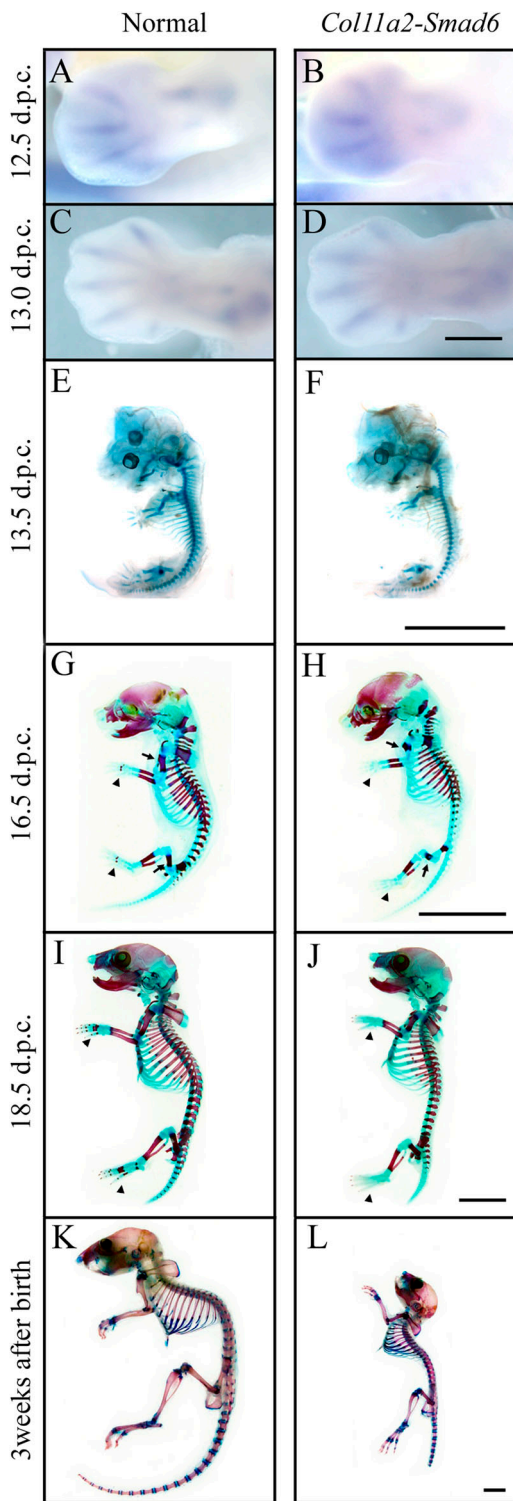
Normal   *Col11a2-Smad6*

12.5 d.p.c.

13.0 d.p.c.

13.5 d.p.c.

16.5 d.p.c.

18.5 d.p.c.

3weeks after birth

Figure 5. **Skeletal development of Smad6 transgenic mice.** (A–D) Whole-mount in situ hybridization using *Col2a1* antisense cRNA probe at 12.5 (A and B) and 13.0 (C and D) d.p.c. (E–L) Alcian blue and Alizarin red S staining of whole skeleton of normal (E, G, I, and K) and transgenic (F, H, J, and L) mice at various stages of development. Arrowheads indicate metatarsals. Arrows show mineralized tissues in humerus and femur. Bars: (A–D) 200 μm; (E–L) 2 mm.

entiation into hypertrophic chondrocytes at the center of each skeletal component (Fig. 6 C). On the other hand, transgenic cartilage from the humerus contained prolifera-

tive but not hypertrophic chondrocytes (Fig. 6 D). Hybridization in situ showed that proliferative chondrocytes in Smad6 transgenic mice expressed *Col2a1* mRNA (Fig. 6 F), like those of normal mice. Northern blotting of limb bud extracts showed that expression levels of the Sox9 gene, *Col2a1*, and type IX collagen α1 chain mRNAs were similar between transgenic and normal mice at 13.5–19.5 d.p.c. (unpublished data). However, the transgenic cartilage lacked type X collagen–positive (Fig. 6 H) and osteopontin-positive (Fig. 6 J) cells, whereas cartilage from normal mice expressed these genes (Fig. 6, G and I). In addition, von Kossa staining revealed mineralization in the normal (Fig. 6 K) but not in the transgenic (Fig. 6 L) mouse humerus. At 16.5 d.p.c., normal mice formed ossification centers in the humerus (Fig. 6 M). However, although a zone of hypertrophic chondrocytes was present in the transgenic humerus, an ossification center had not formed (Fig. 6 N). At 18.5 d.p.c., the transgenic skeletal element was composed of cartilage at both ends and bone at the center, like the wild type (Fig. 6, O and P). These results suggest that Smad6 overexpression delayed chondrocyte hypertrophy and ossification by ∼3 d during development of the mouse humerus.

Normal chondrocyte proliferation and reduced population of hypertrophic chondrocytes in Smad6 transgenic mice

For further analysis of chondrocyte proliferation in Smad6 transgenic mice, we performed BrdU labeling at embryonic (Fig. 7, A and B) and postnatal (Fig. 7, C–F) stages. There were not significant differences in BrdU labeling indexes between chondrocytes of normal and Smad6 transgenic mice at 16.5 d.p.c. (Fig. 7 G) and at 3 wk of age (Fig. 7 H).

Once hypertrophic chondrocytes formed at later stages of development, populations of hypertrophic chondrocytes of transgenic mice did not significantly differ from those of normal littermates (Fig. 7, I, J, and M). However, populations of hypertrophic chondrocytes in Smad6 transgenic mice decreased after birth (Fig. 7, K and L). The mean height of zones of hypertrophic chondrocytes was significantly less than that of normal littermates at 3 wk after birth (Fig. 7 N).

Chondrocyte hypertrophy induced by BMP2 was down-regulated in cartilage explants prepared from Smad6 transgenic mice

To investigate BMP signaling in chondrocytes, we organ cultured primordial metatarsal cartilage at 15.0 d.p.c. Phase-contrast microscopy could distinguish the zones of proliferative and mineralized hypertrophic cartilage in the cultures (Fig. 8 A), which was confirmed by histology (Fig. 8, B and C). At the start of culture, metatarsal rudiments from Smad6 transgenic mice were indistinguishable from those of normal mice (Fig. 8, D and E). After 4 d of culture in control medium, the length of hypertrophic cartilage in normal rudiments was increased (Fig. 8 F), whereas transgenic rudiments lacked hypertrophic cartilage (Fig. 8 G). Culture in the presence of rhBMP2 resulted in excessive outgrowth of the proliferative cartilage at both ends of the rudiments and enhanced formation of a hypertrophic center in the normal
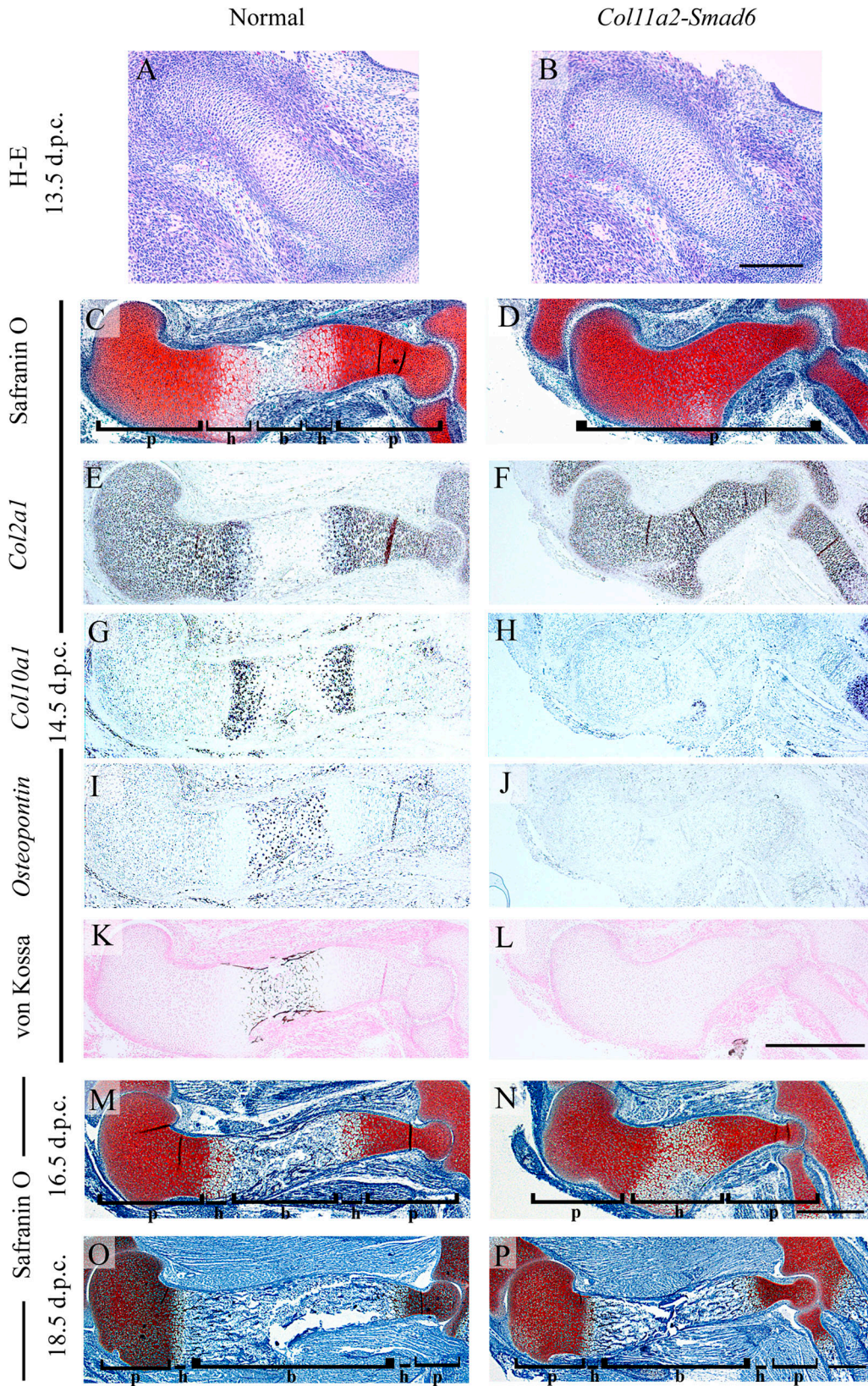
Figure 6.   **Delayed hypertrophy of chondrocytes in Smad6 transgenic mice.** Histology of humerus of normal (A, C, E, G, I, K, M, and O) and Smad6 transgenic (B, D, F, H, J, L, N, and P) mice at various stages of development visualized by hematoxylin and eosin (A and B), safranin O/fast green/iron hematoxylin (C, D, and M–P), and von Kossa (K and L) staining. Semi-serial sections to C and D were hybridized with cRNA probes for *Col2a1* (E and F), *Col10a1* (G and H), and osteopontin gene (I and J). p, Proliferative cartilage; h, hypertrophic cartilage; b, bone. Bars: (A and B) 200 μm; (C–P) 500 μm.
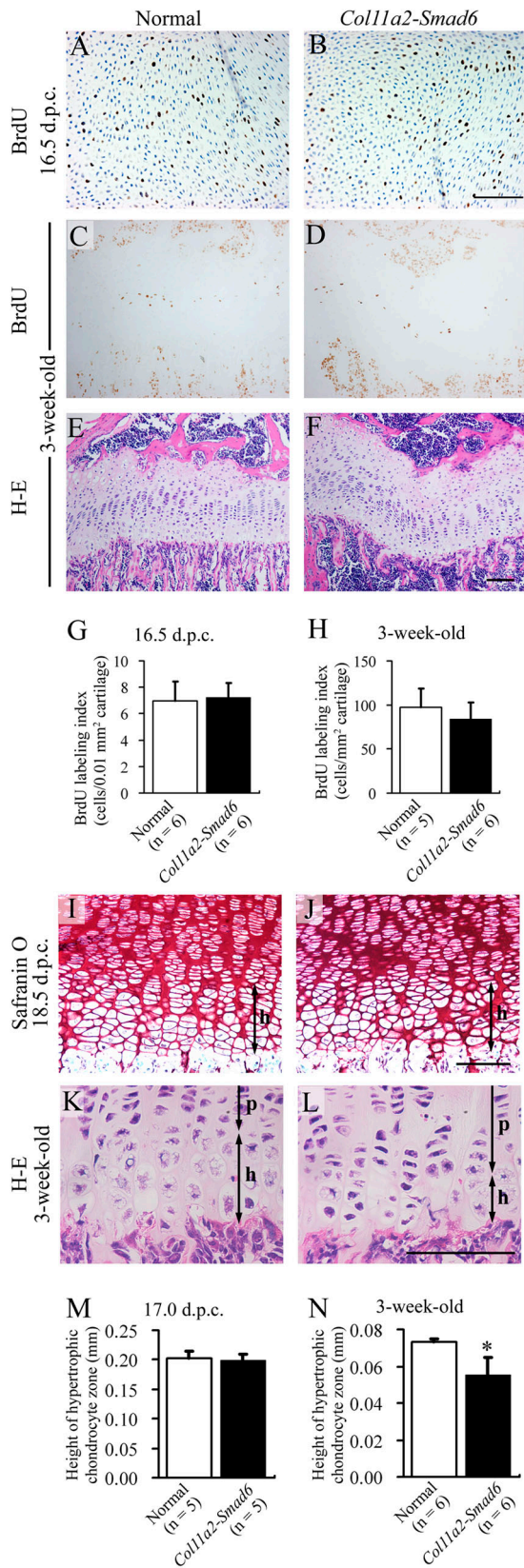
Figure 7. Normal chondrocyte proliferation and reduced population of hypertrophic chondrocytes in Smad6 transgenic mice. (A–D) Immunohistochemical detection of BrdU-labeled chondrocytes in proximal humerus. Proliferative chondrocytes of normal (A) and Smad6 transgenic (B) embryos at 16.5 d.p.c.; counterstained with hematoxylin (A and B). Growth plate cartilage of normal (C) and Smad6 transgenic (D) mice at 3 wk of age. (E and F) Serial sections to C and D were stained with hematoxylin and eosin. Numbers of BrdU-positive cells/mm^2 cartilage compared between normal and transgenic mice at 16.5 d.p.c. (G) and at 3 wk of age (H). (I–L) Zone of hypertrophic chondrocytes of proximal humerus in normal (I and K) and Smad6 transgenic (J and L) mice. Staining with safranin O/fast green/iron hematoxylin at 18.5 d.p.c. (I and J). Staining with hematoxylin and eosin (K and L). Heights of zone of hypertrophic chondrocytes were measured and compared between normal and transgenic mice at 17.0 d.p.c. (M) and at 3 wk of age (N). Error bars show means ± SD. p, Proliferative cartilage; h, hypertrophic cartilage. *, P < 0.001 between normal and transgenic mice as determined by t test. Bars (A–F and I–L), 100 µm.

rudiments (Fig. 8 H). In transgenic rudiments incubated with rhBMP2, proliferative cartilage expanded (Fig. 8 I) like that of normal mice (Fig. 8 H), but formation of the hypertrophic center was limited (Fig. 8 I) compared with that of normal mice (Fig. 8 H). These findings were confirmed by morphometric analysis of the rudiments (Fig. 8, J and K), indicating that Smad6 overexpression inhibited chondrocyte hypertrophy induced by rhBMP2.

The overexpression of Smurf1 in Smad6/Smurf1 double-transgenic mice enhanced phenotypes of Smad6 transgenic mice

To investigate in vivo function of Smurf1, we generated transgenic mice overexpressing Smurf1 in chondrocytes. We prepared the transgene construct by ligating Smurf1 cDNA with a 5′ FLAG epitope to *Col11a2* promoter/enhancer sequences (*Col11a2-Smurf1*; Fig. 9 A). Smurf1 transgenic mice appeared normal in all respects, as they grew normally after birth and were fertile. Northern blotting demonstrated Smurf1 expression in transgenic limb buds (Fig. 9 B). Transgenic 3-kb Smurf1 mRNA was shorter than endogenous Smurf1 mRNA due to differences at both the 5′ and 3′ untranslated regions. Exogenous rhBMP2 added to Smurf1 transgenic cartilage in organ cultures of metatarsal rudiments at 15.0 d.p.c. caused proliferative cartilage outgrowth and hypertrophic center formation as in normal mice. The mean area of proliferative cartilage in Smurf1 transgenic rudiments (0.44 ± 0.03 mm^2) did not significantly differ from that of normal littermates (0.47 ± 0.07 mm^2; n = 6, P = 0.08). The mean length of hypertrophic cartilage in Smurf1 transgenic rudiments (0.26 ± 0.02 mm) also did not significantly differ from that of normal littermates (0.26 ± 0.01 mm; n = 6, P = 0.75). These results suggest that Smurf1 overexpression does not significantly affect either chondrocyte proliferation or hypertrophy induced by rhBMP2.

We then produced transgenic offspring overexpressing both Smad6 and Smurf1 in chondrocytes (Smad6/Smurf1 double-transgenic mice) by mating Smurf1 transgenic mice with Smad6 transgenic mice of line 199 to test cooperative function of Smad6 and Smurf1. The phenotypes of the double-transgenic mice were similar to but more severe than those of Smad6 transgenic mice. At 16.5 d.p.c., mineralization was evident in the metatarsals of normal and Smurf1 transgenic mice (Fig. 9, C and D, arrowheads), but not in Smad6 transgenic and Smad6/Smurf1 double-transgenic mice (Fig. 9, E and F, arrowheads). The mineralized area in
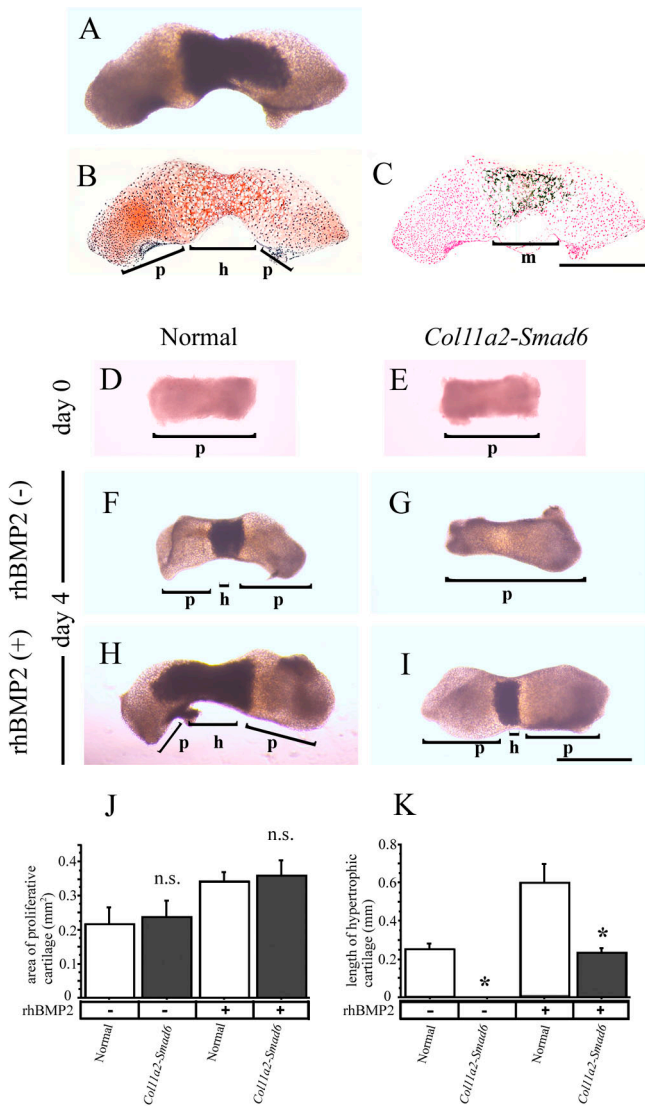
Figure 8. **Down-regulation of chondrocyte hypertrophy induced by rhBMP2 in cartilage explants by Smad6 overexpression.** (A–C) Microscopic and histological appearance of normal mouse metatarsal rudiments cultured in the presence of rhBMP2. (A) Rudiments consist of bright gray areas at both ends and dark gray central areas under phase-contrast microscopy. (B) Histological section stained with safranin O shows that bright and dark gray areas correspond to proliferative and hypertrophic cartilage, respectively. (C) von Kossa staining shows that dark gray areas contain mineralized tissue. (D–I) Cultured metatarsal rudiments prepared from normal (D, F, and H) and Smad6 transgenic (E, G, and I) mice. (D and E) Rudiments at the start of culture. (F and G) Rudiments cultured for 4 d in control medium. (H and I) Rudiments cultured for 1 d in control medium followed by 3 d in medium containing rhBMP2. (J and K) Morphometric analysis of metatarsal explant. Areas of proliferative cartilage and length of hypertrophic cartilage were measured for each rudiment. Error bars show means ± SD ($n = 5$). p, Proliferative cartilage; h, hypertrophic cartilage; m, mineralized hypertrophic cartilage; n.s., not significant. *, $P < 0.01$ between normal and transgenic mice as determined by one-way analysis of variance (ANOVA) followed by Fisher's PLSD test. Bars (A–I), 500 μm.

the femur was significantly shorter in Smad6 transgenic mice than in normal mice. Furthermore, the mineralized area in the femur was significantly shorter in Smad6/Smurf1 double-transgenic mice than in Smad6 transgenic mice.

(Fig. 9, C–G). Histological analysis revealed that ossification was further delayed in the double-transgenic mice compared with the Smad6 transgenic mice (Fig. 9, H and I). Labeling cartilage with BrdU revealed little differences in chondrocyte proliferation among normal littermates and the single- or double-transgenic mice. The labeling indexes at 16.5 d.p.c. were 7.66 ± 1.51, 7.86 ± 1.05, 7.65 ± 1.12, and 7.31 ± 3.74 cells/0.01 mm^2 cartilage in normal littermates, Smurf1 transgenic, Smad6 transgenic, and Smad6/Smurf1 double-transgenic mice, respectively (no significant difference; $n = 5$, $P > 0.05$).

Discussion

Smad6 controls chondrocyte hypertrophy by down-regulating BMP signals in endochondral ossification

Mice lacking Smad6 develop cardiovascular abnormalities (Galvin et al., 2000). Ectopic endochondral bone forms in the heart of mutant mice, suggesting that Smad6 plays certain roles in endochondral bone formation in vivo. However, the physiological roles of Smad6 and Smad signaling in normal endochondral bone formation are poorly understood. In this work, we generated transgenic mice over-expressing Smad6 in chondrocytes. Smad6 overexpression resulted in a delayed chondrocyte hypertrophy and mineralization in endochondral ossification. Smad1/5/8 phosphorylation was inhibited in Smad6 transgenic cartilage, suggesting that Smad signaling was impaired in these mice.

Smad6 appears to block BMP signaling, whereas Smad7 blocks that of both TGF-β and BMP (Hanyu et al., 2001). Skeletal mineralization is delayed and skeletal patterning is defective in mice lacking growth and differentiation factor 5 (Storm et al., 1994), BMPR-IB (Yi et al., 2000), or BMP7 (Luo et al., 1995; Jena et al., 1997). The similarity of delayed mineralization between these mutant mice and Smad6 transgenic mice suggests that BMP signals are blocked by Smad6 during endochondral ossification. This notion was confirmed by our results that chondrocyte hypertrophy and mineralization induced by rhBMP2 was inhibited in cartilage explants from Smad6 transgenic mice. Because the phosphorylation of Smad1/5/8 induced by rhBMP2 was inhibited in explants from Smad6 transgenic mice, we concluded that Smad6 regulates chondrocyte hypertrophy through the inhibition of Smad1/5/8 phosphorylation, thus down-regulating BMP signaling in endochondral bone formation.

The most fundamental abnormality during chondrocyte differentiation in Smad6 transgenic mice was a delay in chondrocyte hypertrophy in humeri at 14.5 d.p.c. This delay was accompanied by the persistent expression of the *Col2a1* gene and the retarded expression of the type X collagen gene (*Col10a1*). Extensive analyses in vitro have shown that BMP signals promote chondrocyte hypertrophy, and BMP-responsive cis-acting elements have been identified in the promoter sequence of the *Col10a1* gene (Volk et al., 1998; Drissi et al., 2003). These in vitro analyses and our in vivo results collectively suggest that Smad6 overexpression blocks BMP signaling, thus preventing transcriptional activation of the *Col10a1* gene.
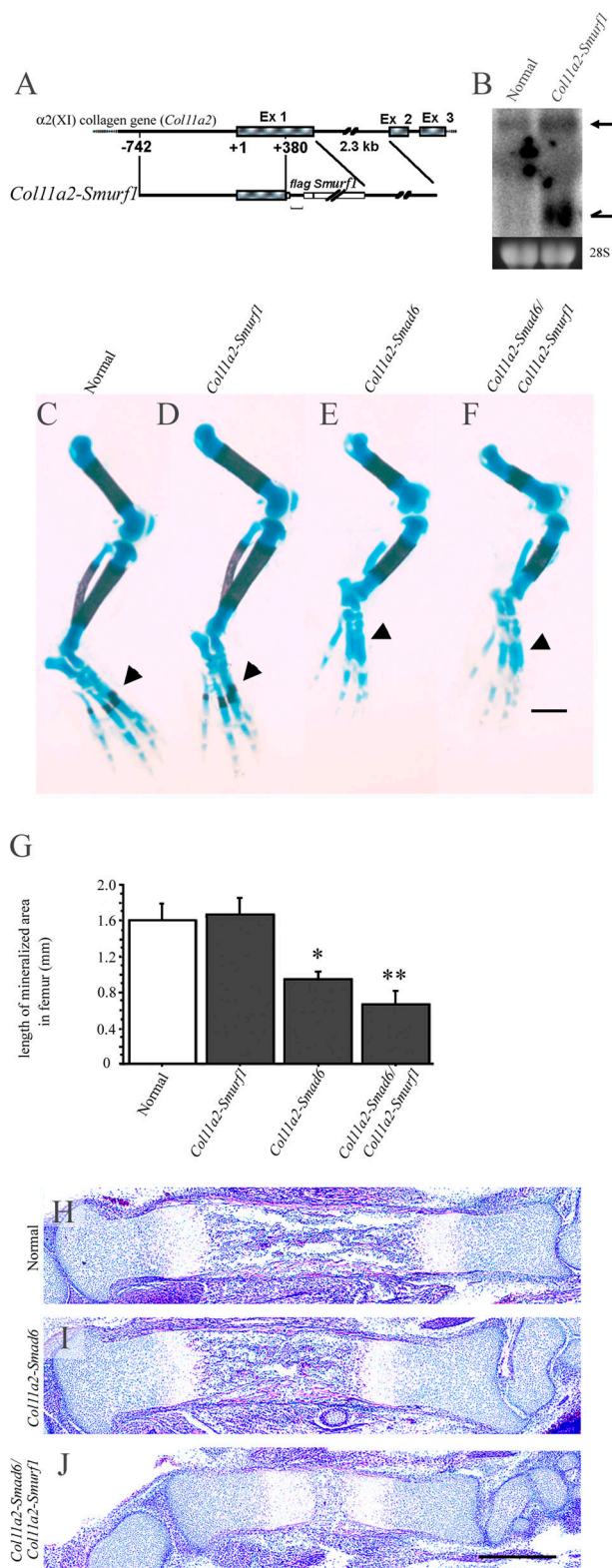
Smad6 regulates endochondral ossification in cooperation with Smurf1

Smurf1 binds Smads 1 and 5 and promotes their degradation (Zhu et al., 1999). Smurf1 and Smad6 form complexes and inhibit BMP signaling through the ubiquitin-dependent degradation of BMP receptors as well as of R-Smads (Murakami et al., 2003). Smurf2 may also exhibit functions similar to Smurf1. To examine the in vivo function of Smurf1, we generated transgenic mice expressing Smurf1 in chondrocytes and did not find obvious abnormalities. These results suggest that sufficient Smurf1 already exists in normal chondrocytes. When apparently normal Smurf1 transgenic mice were mated with Smad6 transgenic mice, the endochondral ossification of progenies overexpressing both Smad6 and Smurf1 was more delayed than in transgenic mice overexpressing only Smad6. It is likely that the Smad6 transgenic mice have far less Smurf1/2 than Smad6. In Smad6/Smurf1 double-transgenic mice, Smurf1 derived from the transgene might compensate for this shortage, thus supporting the activities of a large amount of Smad6. When Smurf1 transgenic mice were mated with those of the Smad6 transgenic line 165 in which the expression level was low, the phenotypic severity of the resultant double-transgenic progeny did not differ from those of Smad6 transgenic mice of line 165 (unpublished data). In Smad6 transgenic mice of this line, endogenous Smurf1/2 fully supported the activities of endogenous Smad6 and that derived from the transgene. From these lines of discussion, the expression level of Smad6 appears to be critical in the regulation of conversion from proliferative chondrocytes to hypertrophic chondrocytes. Actually, the expression level of Smad6 is decreased in the transitional zone between proliferative chondrocytes and hypertrophic chondrocytes (Flanders et al., 2001), suggesting that critical regulation of Smad6 expression is responsible for this conversion. The expression level of inhibitory Smads seems to be consistently and strictly regulated through autoregulatory negative feedback during signal transduction of the TGF-β/BMP superfamily because the inhibitory Smad mRNA is induced by TGF-β stimulation (Heldin et al., 1997).

Postnatal dwarfism with osteopenia might be associated with the reduced zone of hypertrophic chondrocytes

The most apparent phenotype of Smad6 transgenic mice was postnatal dwarfism and osteopenia. Dynamic bone histomorphometric analysis revealed that osteoblastic bone formation decreased and that osteoclastic bone resorption increased in Smad6 transgenic mice. However, results from cultured bone marrow cells suggested normal osteoclast-sup-

Figure 9. **Skeletal phenotypes are more severely disrupted in Smad6/ Smurf1 double-transgenic mice than in Smad6 transgenic mice.** (A) DNA constructs used to generate Smurf1 transgenic mice. Gene structure of *Col11a2* is shown at top. (B) Northern blot hybridized with Smurf1 probe. Left, wild-type; right, Smurf1 transgenic mice. Bottom shows ethidium bromide–stained gel before transfer. (C–F) Alcian blue and Alizarin red S staining of hindlimb skeleton of normal (C), Smurf1 transgenic (D), Smad6 transgenic (E), and Smad6/ Smurf1 double-transgenic (F) mice at 16.5 d.p.c. (G) Length of mineralized area in femur at 16.5 d.p.c. Length of tissue stained with Alizarin red S was measured. (H–J) Histology of tibia of normal (H), Smad6 transgenic (I), and Smad6/Smurf1 double-transgenic (J) mice at 16.5 d.p.c. Arrow shows endogenous Smurf1 mRNA. Half-arrow indicates Smurf1 transgene mRNA. Arrowheads indicate mineralized tissues in metatarsals. Error bars show means ± SD ($n = 5$). *, $P < 0.01$ between normal and Smad6 transgenic mice; **, $P < 0.01$ between Smad6 transgenic and Smad6/Smurf1 double-transgenic mice as determined by one-way analysis of variance (ANOVA) followed by Fisher's PLSD test. Bars (C–F and H–J), 0.5 mm.

porting activities of osteoblasts/stromal cells prepared from Smad6 transgenic mice. These in vitro results suggest that the increased in vivo osteoclastic bone resorption in transgenic mice was not due to an autonomous abnormality within bone marrow cells. This notion was consistent with the observation that the transgene was specifically expressed in chondrocytes. We speculate that abnormal activities of osteoblasts and osteoclasts might be associated with the dysfunction in cartilage during endochondral bone formation. However, we could not rigorously exclude leaky transgene expression in cells in osteoblast lineage, and thus the possibility that osteoblasts have a primary malfunction.

BrdU labeling revealed that proliferation of chondrocytes in Smad6 transgenic mice was normal at the embryonic stage and at the postnatal stage. Therefore, postnatal dwarfism in Smad6 transgenic mice might develop through a different mechanism from that in transgenic mice overexpressing activated FGF receptor 3 in cartilage, in which chondrocyte proliferation is normal in embryos but postnatally decreased (Naski et al., 1998).

The onset of chondrocyte hypertrophy was delayed by $\sim$3 d during the development of Smad6 transgenic mice. Once the zone of hypertrophic chondrocytes formed, the height of the zone of hypertrophic chondrocytes was essentially normal, suggesting that the population of hypertrophic chondrocytes is strictly regulated at late embryonic stages. We did not determine which mechanism maintains the population of hypertrophic chondrocytes in Smad6 transgenic embryos. However, this population decreased in the transgenic mice after birth. It is likely that reduced hypertrophic chondrocyte population lead to a deficiency in signals required for coordination of growth and bone formation after birth. Hypertrophic chondrocytes are known to produce various factors, including angiogenic factors (Karsenty and Wagner, 2002). A reduction in production of such factors may well lead to dysfunction of osteoblast/osteoclast activities, thus resulting in impaired bone growth and osteopenia.

It is also possible that abnormal chondrocyte hypertrophy could result in the impaired structure of the ECM of hypertrophic cartilage. An impaired matrix might not provide a suitable scaffold for osteoblasts and osteoclasts to replace cartilage with bone. This speculation remains to be examined.

Chondrocyte proliferation was not affected in Smad6 transgenic mice

Previously, we generated transgenic mice expressing noggin in chondrocytes under the control of the identical *Col11a2* promoter/enhancer sequences used in this paper (Tsumaki et al., 2002). We examined 62 G_0 founder mouse embryos for the noggin transgene, and 7 of them displayed a severe phenotype and almost completely lacked cartilage formation during development. On the other hand, 17 of 129 G_0 embryos were genetically positive for the Smad6 transgene, and skeletal abnormalities were either relatively minor or almost absent. Although we could not exclude the possibility that the phenotypic difference between noggin and Smad6 transgenic mice might be related to the different level of expression of the transgenes, these results suggest that noggin tends to affect cartilage more than Smad6 when expressed in chondrocytes in transgenic mice.

In addition, chondrocyte proliferation is inhibited in mice lacking BMPR-IB (Yi et al., 2000) and in cartilage explants cultured in the presence of noggin (Minina et al., 2001). Reports have consistently indicated that BMP signaling stimulates chondrocyte proliferation during endochondral bone formation at the embryonic stages of transgenic mice overexpressing BMPs in cartilage (Tsumaki et al., 1999, 2002) and in organ culture of cartilage rudiments in the presence of BMPs (De Luca et al., 2001; Minina et al., 2001).

On the other hand, chondrocyte proliferation appeared normal in Smad6 transgenic mice, as indicated by BrdU labeling. For explanation of the discrepancy between the findings of chondrocyte proliferation obtained from Smad6 transgenic mice and those of other papers, we considered four possibilities. First, we could not exclude the possibility that the expression level of Smad6 transgene was not sufficient to block BMP signaling completely, although immunohistochemical analysis showed strong expression of the transgene (Fig. 2, C–J) Second, Smad signaling might not be blocked by Smad6 alone. Certainly, phenotypes of Smad6/Smurf1 double-transgenic mice were more severe than that of Smad6 transgenic mice. However, it is still milder than that of noggin transgenic mice, and chondrocyte proliferation remained normal, as indicated by BrdU labeling. Third, BMP signals might be mediated by signaling pathways other than Smad proteins. In certain cell types, various MAPKs have been reported to mediate BMP pathways (Iwasaki et al., 1999). Existence of such pathways might account for the discrepancy between chondrocyte proliferation in BMPR-IB–deficient mice and Smad6 transgenic mice. There is likelihood of the fourth possibility as follows: BMPs and noggin are secreted and diffuse. In addition to direct binding to chondrocytes, these proteins might exert indirect effects on chondrocytes. For example, BMPs act on cells around cartilage, and in return these cells secrete factors, affecting chondrocyte proliferation. Thus, the addition or overexpression of BMPs/noggin modulate chondrocyte proliferation directly and indirectly. On the other hand, Smad6 overexpression in chondrocytes might block only the direct effect of BMPs on chondrocytes.

In conclusion, our data on inhibition of endochondral bone formation in Smad6 and Smurf1 transgenic mice suggest a role for Smad signaling in skeletogenesis and growth. By down-regulating Smad1/5/8 phosphorylation and BMP signals, Smad6 plays an important role in regulation of chondrocyte hypertrophy and synergistically cooperates with Smurf1 in vivo.

Materials and methods

Construction of the transgene

The $\alpha2$(XI) collagen gene–based expression vector, 742*lacZ*Int, contains the *Col11a2* promoter (-742 to $+380$), an SV40 RNA splice site, the β-galactosidase reporter gene, the SV40 polyadenylation signal, and 2.3 kb of the first intron sequence of *Col11a2* as an enhancer (Tsumaki et al., 1996). To create a Smad6 transgene, a 1.5-kb DNA fragment covering the entire coding region of mouse Smad6 cDNA tagged with a FLAG sequence at the NH_2 terminus was prepared. The FLAG-tagged Smad6 cDNA was cloned into the NotI sites of 742*lacZ*Int expression vectors by replacing the β-galactosidase gene to create *Col11a2-Smad6*. For the Smurf1 transgene, a FLAG-tagged Smurf1 cDNA was cloned into NotI sites of the expression vectors 742*lacZ*Int by replacing the β-galactosidase gene to create *Col11a2-Smurf1*.

Generation of transgenic mice

The plasmids *Col11a2-Smad6* and *Col11a2-Smurf1* were digested with EcoRI and PstI to release the inserts. Transgenic mice were produced by microinjecting each of the inserts into the pronuclei of fertilized eggs from F1 hybrid mice (C57BL/6x DBA) as described previously (Tsumaki et al., 1996). Transgenic embryos were identified by PCR assays of genomic DNA extracted from the placenta or skin. Genomic DNA was amplified by transgene-specific PCR using primers derived from mouse Smad6 cDNA (5′-CAAGATCGGTTTTGGCATACTG-3′) and from the SV40 poly(A) signal region (5′-TCACTGCATTCTAGTTGTGGTTTGTCC-3′) to amplify a 411-bp product for Smad6 transgenic mice. To discriminate Smurf1 transgenic mice, genomic DNA was amplified by transgene-specific PCR using primers derived from mouse Smurf1 cDNA (5′-ATGGACTACAAGGACGAT-GATGACAAGG-3′ and 5′-AGGGGCTGGTTCCTCCATGAAGCAG-3′) to amplify a 570-bp product. Smad6/Smurf1 double-transgenic pups were generated by mating Smad6 and Smurf1 transgenic mice.

Staining of the skeleton

Mice were dissected and fixed in 100% ethanol overnight, and then stained with Alcian blue followed by Alizarin red S solution according to standard protocols (Peters, 1977).

Micro CT analysis and bone mass measurement

The humeri from 5-wk-old transgenic mice and normal littermates were dissected and analyzed using a micro-focus X-ray CT system (SMX-100CT-SV; Shimadzu). The region extending from the proximal growth plate to the metaphyseal part of the humerus on 350 slices was scanned at a width of 6.75 μm per slice. The data were reconstructed to produce images of the humerus using 3-D visualization and measurement software (Vay Tek, Inc.). Bone mass was quantified by selecting 90 consecutive slices distal to the proximal growth plate (0.6 mm in length). Trabecular parameters in the metaphysis were determined using image analysis software (TRI/3D-BON; RATOC).

Histology and immunohistochemical staining

Embryos were dissected using a stereomicroscope (model SMZ645; Nikon), fixed in 4% PFA, processed, and embedded in paraffin. Serial sections were stained with hematoxylin and eosin, with safranin O/fast green/iron hematoxylin, or by the von Kossa reaction. Dynamic histomorphometric indices were determined by double-fluorescence labeling in vertebral bodies. 4-wk-old normal and transgenic mice were administered i.p. with tetracycline (20 mg/kg body weight; Sigma-Aldrich), followed by calcein label (10 mg/kg body weight; Wako Chemicals) 2 d later. After 24 h, the mice were killed. Bones were fixed with ethanol and embedded in methylmethacrylate. Sections were cut and viewed using a fluorescence microscope (Eclipse E1000; Nikon). The Niigata Bone Science Institute (Niigata, Japan) performed histomorphometric analyses. Immunohistochemistry proceeded using a rabbit pAb against Smad6 (1:200 dilution; Zymed Laboratories) and a rabbit pAb against phospho-Smad1/5/8 (1:200 dilution; Cell Signaling Technology). Immune complexes were detected using streptavidin-peroxidase staining and Histofine SAB-PO kits (Nichirei). Images were acquired using a microscope (Eclipse E1000; Nikon) with a digital camera system (DXM1200; Nikon).

BrdU staining

Pregnant mice bearing 16.5 d.p.c. embryos and 3-wk-old mice were i.p. injected with BrdU labeling reagent (10 μl/g body weight; Zymed Laboratories). 2 h later, the mice were killed. Embryonic limb buds and tibia of the 3-wk-old mice were dissected and sectioned. Incorporated BrdU was detected using a BrdU staining kit (Zymed Laboratories) to distinguish actively proliferating cells. Tissue sections were measured using a micrometer, and the average number of BrdU-positive cells/mm^2 cartilage ± SD was calculated.

Northern hybridization and real-time quantitative RT-PCR

Total RNA extracted from the limb buds of 14.5–18.5 d.p.c. transgenic and normal embryos using RNeasy Mini Kits (QIAGEN) was fractionated by electrophoresis through formaldehyde agarose gels and transferred onto Nytran® membranes (Schleicher & Schuell Bioscience). Complementary DNAs (cDNAs) were labeled with [^{32}P]dCTP using Prime-it® II kits (Stratagene). The membranes were hybridized with ^{32}P-labeled Smad6 cDNA and rehybridized with ^{32}P-labeled probes for mouse α1(II) collagen, α1(IX) collagen, and *Sox9*.

Total RNAs were digested with DNase to eliminate any contaminating genomic DNA before real-time quantitative RT-PCR. 2 μg of total RNA was reverse transcribed into first-strand cDNA using OmniScript® reverse transcriptase (QIAGEN) and an oligo(dT)12-18 primer. The PCR amplification proceeded in 20 μl containing 1 μl of cDNA, 2 μl of SYBER Green™ Master Mix (QIAGEN), and 10 pmol of primers specific for Smad6 (5′-GATCCCCAAGCCAGACAGT-3′ and 5′-AGCCTCTTGAGCAGCGC-GAGTA-3′) to generate a 126-bp product (GenBank/EMBL/DDBJ accession no. NM008542). The cDNA was amplified by 35 cycles using a LightCycler® quick system (Roche) according to the following protocol: 94°C for 15 s, 60°C for 20 s, and 72°C for 6 s, each with a temperature transition rate of 20°C, according to the manufacturer's instructions.

In situ hybridization

Digoxigenin-11 UTP-labeled single-strand RNA probes were prepared using a DIG RNA labeling kit (Boehringer) according to the manufacturer's instructions. We generated antisense and sense probes using α1(II) collagen, α1(X) collagen, and osteopontin cDNAs. Hybridization proceeded as described previously (Hirota et al., 1992; Conlon and Herrmann, 1993). A Genius detection system (Boehringer) detected signals according to the manufacturer's instructions.

Immunoprecipitation and Western blotting

Limb buds of 14.5 d.p.c transgenic and normal embryos were lysed with RIPA buffer (50 mM Tris, pH 7.4, 150 mM NaCl, 1% Nonidet P-40, 0.5% sodium deoxycholate, 0.1% SDS, and 10 mM DTT) supplemented with protease and phosphatase inhibitor cocktails (Sigma-Aldrich). The positive control consisted of COS7 cells transfected with the expression construct FLAG-Smad6 that was also lysed with RIPA buffer. The cell lysates were incubated with anti-Smad6 antibody (Zymed Laboratories) for 3 h at 4°C followed by an incubation with protein G–agarose beads (Roche) for 3 h at 4°C. After five washes with lysis buffer (20 mM Hepes, 150 mM NaCl, 10% glycerol, 1.5 mM MgCl$_2$, 1 mM EGTA, and 100 μM orthovanadate), 1× SDS sample buffer was added to the agarose beads. The samples were incubated for 5 min at 95°C, fractionated by 10% SDS-PAGE, transferred onto nitrocellulose membranes (Bio-Rad Laboratories), and Western blotted against anti-FLAG M2 mAb (Sigma-Aldrich). Immunocomplex bands were visualized using the ECL Western blotting detection system (Amersham Biosciences).

Bone marrow cell culture

Osteoclast formation and bone resorbing activity were determined using the modified method described in Azuma et al. (2000). In brief, bone marrow cells prepared from the femurs and tibias of 10-wk-old transgenic mice or wild-type control mice were suspended in α-modified essential medium containing 10% FBS, and were cultured in 48-well plates (10^6 cells/0.5 ml per well) for 7 d in the presence of 0.1 μM dexamethasone (Sigma-Aldrich) and 0.01 μM recombinant human parathyroid hormone (Peptide Institute, Inc.). Cells were then fixed and stained for TRAP using a TRAP staining kit (Hokudo) according to the manufacturer's recommendation. The number of multinucleated TRAP-positive cells with more than three nuclei was counted under a microscope (Eclipse TE300; Nikon). To examine calcified matrix resorption activity, 5 × 10^5 cells were cultured in 16-well hydroxyapatite-coated slides (Osteologic; Becton Dickinson) for 14 d, and the resorption area was calculated by computer-assisted image analysis.

Metatarsal explant culture

Metatarsal rudiments were cultured as described previously (Haaijman et al., 1997). Metatarsal rudiments were dissected from transgenic and normal embryos at 15.0 d.p.c. and cultured in α-modified essential medium without nucleosides (Invitrogen), supplemented with 0.05 mg/ml ascorbic acid (Sigma-Aldrich), 0.3 mg/ml L-glutamine (Merck), 0.05 mg/ml gentamycin (Invitrogen), 0.25 mg/ml Fungizone® (Invitrogen), 1 mM β-glycerophosphate (Merck), and 0.2% FBS (GIBCO BRL) in a humidified atmosphere of 5% CO$_2$ in air at 37°C. 1 d after starting the cultures, the rudiments were incubated in 400 μl of the same medium containing 500 ng/ml of rhBMP2 (Yamanouchi Pharmaceutical Co., Ltd.) or without rhBMP2 for a further 3 d. For immunohistochemical analysis using anti-phosphorylated Smad1/5/8, rudiments were sectioned before and after a 2-h incubation with rhBMP2. Images of rudiments obtained under inverted phase-contrast microscopy were analyzed morphometrically (Eclipse TE300; Nikon). Areas of proliferative cartilage and length of hypertrophic cartilage were measured using NIH Image software (National Institutes of Health, Bethesda, MD).

———————

References

Azuma, Y., K. Kaji, R. Katogi, S. Takeshita, and A. Kudo. 2000. Tumor necrosis factor-α induces differentiation of and bone resorption by osteoclasts. *J. Biol. Chem.* 275:4858–4864.

Balemans, W., and W. Van Hul. 2002. Extracellular regulation of BMP signaling in vertebrates: a cocktail of modulators. *Dev. Biol.* 250:231–250.

Conlon, R.A., and B.G. Herrmann. 1993. Detection of messenger RNA by in situ hybridization to postimplantation embryo whole mounts. *Methods Enzymol.* 225:373–383.

De Luca, F., K.M. Barnes, J.A. Uyeda, S. De-Levi, V. Abad, T. Palese, V. Mericq, and J. Baron. 2001. Regulation of growth plate chondrogenesis by bone morphogenetic protein-2. *Endocrinology.* 142:430–436.

Drissi, M.H., X. Li, T.J. Sheu, M.J. Zuscik, E.M. Schwarz, J.E. Puzas, R.N. Rosier, and R.J. O'Keefe. 2003. Runx2/Cbfa1 stimulation by retinoic acid is potentiated by BMP2 signaling through interaction with Smad1 on the collagen X promoter in chondrocytes. *J. Cell. Biochem.* 90:1287–1298.

Ebisawa, T., M. Fukuchi, G. Murakami, T. Chiba, K. Tanaka, T. Imamura, and K. Miyazono. 2001. Smurf1 interacts with transforming growth factor-β type I receptor through Smad7 and induces receptor degradation. *J. Biol. Chem.* 276:12477–12480.

Erlebacher, A., E.H. Filvaroff, S.E. Gitelman, and R. Derynck. 1995. Toward a molecular understanding of skeletal development. *Cell.* 80:371–378.

Flanders, K.C., E.S. Kim, and A.B. Roberts. 2001. Immunohistochemical expression of Smads 1-6 in the 15-day gestation mouse embryo: signaling by BMPs and TGF-βs. *Dev. Dyn.* 220:141–154.

Galvin, K.M., M.J. Donovan, C.A. Lynch, R.I. Meyer, R.J. Paul, J.N. Lorenz, V. Fairchild-Huntress, K.L. Dixon, J.H. Dunmore, M.A. Gimbrone, Jr., et al. 2000. A role for smad6 in development and homeostasis of the cardiovascular system. *Nat. Genet.* 24:171–174.

Haaijman, A., R.N. D'Souza, A.L. Bronckers, S.W. Goei, and E.H. Burger. 1997. OP-1 (BMP-7) affects mRNA expression of type I, II, X collagen, and matrix Gla protein in ossifying long bones in vitro. *J. Bone Miner. Res.* 12:1815–1823.

Hanyu, A., Y. Ishidou, T. Ebisawa, T. Shimanuki, T. Imamura, and K. Miyazono. 2001. The N domain of Smad7 is essential for specific inhibition of transforming growth factor-β signaling. *J. Cell Biol.* 155:1017–1027.

Heldin, C.H., K. Miyazono, and P. ten Dijke. 1997. TGF-β signalling from cell membrane to nucleus through SMAD proteins. *Nature.* 390:465–471.

Hirota, S., A. Ito, E. Morii, A. Wanaka, M. Tohyama, Y. Kitamura, and S. Nomura. 1992. Localization of mRNA for c-kit receptor and its ligand in the brain of adult rats: an analysis using in situ hybridization histochemistry. *Brain Res. Mol. Brain Res.* 15:47–54.

Hogan, B.L. 1996. Bone morphogenetic proteins: multifunctional regulators of vertebrate development. *Genes Dev.* 10:1580–1594.

Iwasaki, S., M. Iguchi, K. Watanabe, R. Hoshino, M. Tsujimoto, and M. Kohno. 1999. Specific activation of the p38 mitogen-activated protein kinase signaling pathway and induction of neurite outgrowth in PC12 cells by bone morphogenetic protein-2. *J. Biol. Chem.* 274:26503–26510.

Jena, N., C. Martin-Seisdedos, P. McCue, and C.M. Croce. 1997. BMP7 null mu-

tation in mice: developmental defects in skeleton, kidney, and eye. *Exp. Cell Res.* 230:28–37.

Karsenty, G., and E.F. Wagner. 2002. Reaching a genetic and molecular understanding of skeletal development. *Dev. Cell.* 2:389–406.

Kavsak, P., R.K. Rasmussen, C.G. Causing, S. Bonni, H. Zhu, G.H. Thomsen, and J.L. Wrana. 2000. Smad7 binds to Smurf2 to form an E3 ubiquitin ligase that targets the TGF β receptor for degradation. *Mol. Cell.* 6:1365–1375.

Luo, G., C. Hofmann, A.L. Bronckers, M. Sohocki, A. Bradley, and G. Karsenty. 1995. BMP-7 is an inducer of nephrogenesis, and is also required for eye development and skeletal patterning. *Genes Dev.* 9:2808–2820.

Minina, E., H.M. Wenzel, C. Kreschel, S. Karp, W. Gaffield, A.P. McMahon, and A. Vortkamp. 2001. BMP and Ihh/PTHrP signaling interact to coordinate chondrocyte proliferation and differentiation. *Development.* 128:4523–4534.

Murakami, G., T. Watabe, K. Takaoka, K. Miyazono, and T. Imamura. 2003. Cooperative inhibition of bone morphogenetic protein signaling by smurf1 and inhibitory smads. *Mol. Biol. Cell.* 14:2809–2817.

Naski, M.C., J.S. Colvin, J.D. Coffin, and D.M. Ornitz. 1998. Repression of hedgehog signaling and BMP4 expression in growth plate cartilage by fibroblast growth factor receptor 3. *Development.* 125:4977–4988.

Nishihara, A., M. Fujii, T.K. Sampath, K. Miyazono, and A.H. Reddi. 2003. Bone morphogenetic protein signaling in articular chondrocyte differentiation. *Biochem. Biophys. Res. Commun.* 301:617–622.

Olsen, B.R., A.M. Reginato, and W. Wang. 2000. Bone development. *Annu. Rev. Cell Dev. Biol.* 16:191–220.

Peters, P.W.J. 1977. Double staining of fetal skeletons for cartilage and bone. *In* Methods in Prenatal Toxicology. H.J.M.D. Neuberg and T.E. Kwasigroch, editors. Georg Thieme Verlag, Stuttgart, Germany. 153–154.

Shi, Y., and J. Massague. 2003. Mechanisms of TGF-β signaling from cell membrane to the nucleus. *Cell.* 113:685–700.

Storm, E.E., T.V. Huynh, N.G. Copeland, N.A. Jenkins, D.M. Kingsley, and S.J. Lee. 1994. Limb alterations in brachypodism mice due to mutations in a new member of the TGF β-superfamily. *Nature.* 368:639–643.

Tsumaki, N., T. Kimura, Y. Matsui, K. Nakata, and T. Ochi. 1996. Separable cis-regulatory elements that contribute to tissue- and site-specific α2(XI) collagen gene expression in the embryonic mouse cartilage. *J. Cell Biol.* 134:1573–1582.

Tsumaki, N., K. Tanaka, E. Arikawa-Hirasawa, T. Nakase, T. Kimura, J.T. Thomas, T. Ochi, F.P. Luyten, and Y. Yamada. 1999. Role of CDMP-1 in skeletal morphogenesis: promotion of mesenchymal cell recruitment and chondrocyte differentiation. *J. Cell Biol.* 144:161–173.

Tsumaki, N., T. Nakase, T. Miyaji, M. Kakiuchi, T. Kimura, T. Ochi, and H. Yoshikawa. 2002. Bone morphogenetic protein signals are required for cartilage formation and differently regulate joint development during skeletogenesis. *J. Bone Miner. Res.* 17:898–906.

Valcourt, U., J. Gouttenoire, A. Moustakas, D. Herbage, and F. Mallein-Gerin. 2002. Functions of transforming growth factor-β family type I receptors and Smad proteins in the hypertrophic maturation and osteoblastic differentiation of chondrocytes. *J. Biol. Chem.* 277:33545–33558.

Volk, S.W., P. Luvalle, T. Leask, and P.S. Leboy. 1998. A BMP responsive transcriptional region in the chicken type X collagen gene. *J. Bone Miner. Res.* 13:1521–1529.

Yi, S.E., A. Daluiski, R. Pederson, V. Rosen, and K.M. Lyons. 2000. The type I BMP receptor BMPRIB is required for chondrogenesis in the mouse limb. *Development.* 127:621–630.

Zhang, Y., C. Chang, D.J. Gehling, A. Hemmati-Brivanlou, and R. Derynck. 2001. Regulation of Smad degradation and activity by Smurf2, an E3 ubiquitin ligase. *Proc. Natl. Acad. Sci. USA.* 98:974–979.

Zhu, H., P. Kavsak, S. Abdollah, J.L. Wrana, and G.H. Thomsen. 1999. A SMAD ubiquitin ligase targets the BMP pathway and affects embryonic pattern formation. *Nature.* 400:687–693.